

# Synthesis and characterization of biocompatible Fe<sub>3</sub>O<sub>4</sub> nanoparticles

Jing Sun,<sup>1</sup> Shaobing Zhou,<sup>1</sup> Peng Hou,<sup>1</sup> Yuan Yang,<sup>2</sup> Jie Weng,<sup>1</sup> Xiaohong Li,<sup>1</sup> Mingyuan Li<sup>2</sup>

<sup>1</sup>School of Materials Science and Engineering, Key Laboratory of Advanced Technologies of Materials, Ministry of Education, Southwest Jiaotong University, Chengdu 610031, People's Republic of China

<sup>2</sup>Department of Microbiology, Huaxi Basic Medicine and Forensic College, Sichuan University, Chengdu 610041, People's Republic of China

Received 11 January 2006; revised 9 March 2006; accepted 21 March 2006

Published online 25 September 2006 in Wiley InterScience (www.interscience.wiley.com). DOI: 10.1002/jbm.a.30909

**Abstract:** In this study, magnetite (Fe<sub>3</sub>O<sub>4</sub>) nanoparticles with a size range of 8–20 nm were prepared by the modified controlled chemical coprecipitation method from the solution of ferrous/ferric mixed salt-solution in alkaline medium. In the process, two kinds of surfactant (sodium oleate and polyethylene glycol) were studied; then, sodium oleate was chosen as the apt surfactant to attain ultrafine, nearly spherical and well-dispersed (water-base) Fe<sub>3</sub>O<sub>4</sub> nanoparticles, which had well magnetic properties. The size and size distribution of nanoparticles were determined by particle size analyzer. And the magnetite nanoparticles was characterized by X-ray powder diffraction (XRD) analysis, transmission electron microscopy (TEM), electron diffraction (ED) photography, Fourier transform infrared spectrometer (FT-IR), and vibrating-sample magnetometer (VSM). Also

the effect of many parameters on the Fe<sub>3</sub>O<sub>4</sub> nanoparticles was studied, such as reaction temperature, pH of the solution, stirring rate and concentration of sodium oleate. And the 5-dimethylthiazol-2-yl-2,5-diphenyltetrazolium bromide (MTT) assay was performed to evaluate the biocompatibility of magnetite nanoparticles. The results showed that the Fe<sub>3</sub>O<sub>4</sub> nanoparticles coated by sodium oleate had a better biocompatibility, better magnetic properties, easier washing, lower cost, and better dispersion than the magnetite nanoparticles coated by PEG. © 2006 Wiley Periodicals, Inc. *J Biomed Mater Res* 80A: 333–341, 2007

**Key words:** chemical coprecipitation; magnetite; sodium oleate; polyethylene glycol; nanoparticles; surfactant; cytotoxicity

## INTRODUCTION

Recently, considerable research has been focused on iron oxides due to their potential uses such as pigment, magnetic drug targeting, magnetic resonance imaging for clinical diagnosis, recording material and catalyst, etc.<sup>1–3</sup> The magnetic nanoparticles exhibit superparamagnetic behavior because of the infinitely small coercivity arising from the negligible energy barrier in the hysteresis of the magnetization loop of the particles as predicted by Bloch and Neel.<sup>4</sup> There are many various ways to prepare Fe<sub>3</sub>O<sub>4</sub> nanoparticles, which have been reported in other papers, such

as arc discharge, mechanical grinding, laser ablation, microemulsions, and high temperature decomposition of organic precursors, etc.<sup>5</sup> These methods may be able to prepare magnetite with several controllable particle diameters. However, well-dispersed aqueous Fe<sub>3</sub>O<sub>4</sub> nanoparticles have met with very limited success.

As one convenient and cheap method, chemical coprecipitation method has the potential to meet the increasing demand for the direct preparation of well-dispersed (water-base) Fe<sub>3</sub>O<sub>4</sub> nanoparticles and offer a low-temperature alternative to conventional powder synthesis techniques in the production of nanoparticles, and the sizes of nanoparticles can be well controlled by apt surfactant.<sup>6,7</sup> Chemical coprecipitation can produce fine, high-purity, stoichiometric particles of single and multicomponent metal oxides. Furthermore, if process conditions such as solution pH, reaction temperature, stirring rate, solute concentration and surfactant concentration are carefully controlled, oxide particles of the desired shape and sizes can be produced.<sup>8</sup>

In current study, a modified divalent/trivalent iron salts coprecipitation synthesis using aqueous ammo-

Correspondence to: Prof. S. Zhou; e-mail: shaobingzhou@home.swjtu.edu.cn or Prof. J. Weng; e-mail: jweng@home.swjtu.edu.cn

Contract grant sponsor: National Natural Science Foundation of China; contract grant number: 50303018

Contract grant sponsor: Ministry of Education of China

nium hydroxide ( $\text{NH}_3 \cdot \text{H}_2\text{O}$ ) was used to produce  $\text{Fe}_3\text{O}_4$  nanoparticles, which can be well-dispersed in an aqueous solution. In the process, dry nitrogen was used to keep the system under the atmosphere of nonoxygen so as to protect divalent iron salts from oxidation. Also we discussed two kinds of surfactant [sodium oleate and polyethylene glycol (PEG,  $M_w = 6000$ )], which have fine biocompatibility,<sup>9</sup> then sodium oleate was chosen as the apt surfactant and the  $\text{Fe}_3\text{O}_4$  nanoparticles were coated with it for two times, from which the sizes of magnetite can be well controlled. The process can be showed as the following Scheme 1.

## MATERIALS AND METHODS

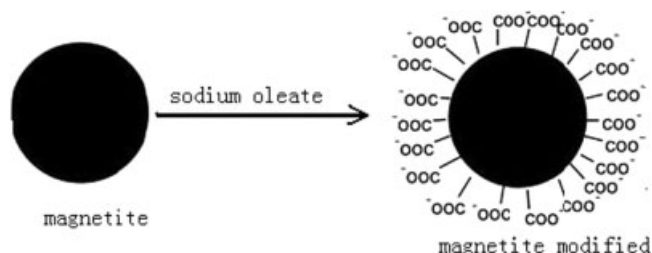
### Initial treatment on reactants

Sodium oleate and polyethylene glycol (PEG,  $M_w = 6000$ ) were purchased from Chengdu KeLong Chemical Reagent Company (SiChuan, China). 3-(4,5-Dimethylthiazol-2-yl)-2,5-diphenyltetrazolium bromide (MTT) was purchased from Sigma. All the other chemicals used in this work were analytical reagent grade from commercial market without further purification. Distilled water was used for preparation of the solutions after deoxygenation with dry  $\text{N}_2$  for 10 min. The divalent ( $\text{FeCl}_2 \cdot 4\text{H}_2\text{O}$ ), trivalent ( $\text{FeCl}_3 \cdot 6\text{H}_2\text{O}$ ) iron salts and aqueous ammonium hydroxide (25–28%, w/w) were also deoxygenated with dry nitrogen before use.

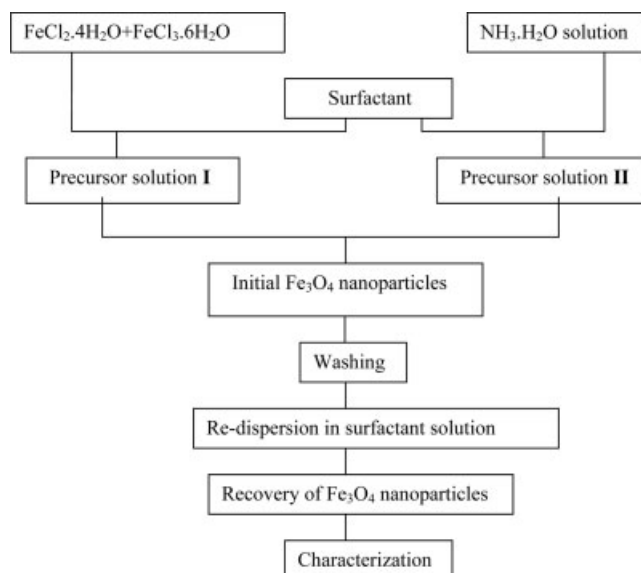
### Preparation of $\text{Fe}_3\text{O}_4$ nanoparticles

The process for preparing  $\text{Fe}_3\text{O}_4$  nanoparticles by controlled chemical coprecipitation is schematically illustrated in Scheme 2.

First, 1.99 g (0.01 mol)  $\text{FeCl}_2 \cdot 4\text{H}_2\text{O}$ , 5.41 g (0.02 mol)  $\text{FeCl}_3 \cdot 6\text{H}_2\text{O}$  was dissolved in 50 mL distilled water, aqueous ammonium hydroxide (25–28%, w/w) solution (1.5 mol/L) was also obtained as this. Then, a certain surfactant (sodium oleate or PEG-6000) was added to the former solutions to obtain Precursor solution II and Precursor solution I. Second, Precursor solution I was added into Precursor solution II dropwise with strong stirring under the protection of dry nitrogen at the desired temperature. Just after mixing the solutions, the color of the solution changed from



**Scheme 1.** The process of magnetite modified by sodium oleate.



**Scheme 2.** Procedure for the preparation of  $\text{Fe}_3\text{O}_4$  nanoparticles by the controlled chemical coprecipitation method.

light brown to black, indicating the forming of  $\text{Fe}_3\text{O}_4$  nanoparticles, which was allowed to crystallize completely for another 60 min under rapid stirring. The precipitate  $\text{Fe}_3\text{O}_4$  nanoparticles were washed by repeated cycles of centrifugation and redispersion in distilled water. Washing was performed for five times in distilled water. Third, the precipitate  $\text{Fe}_3\text{O}_4$  nanoparticles were redispersed in the same surfactant solution under the conditions of ultrasonic agitation for 30 min and strong stirring for another 40 min. The products ( $\text{Fe}_3\text{O}_4$  nanoparticles) were also washed by repeated cycles of centrifugation and redispersion in distilled water. And washing was performed for four times in distilled water. Then, the final products were dried in a vacuum oven at room temperature for 24 h, and the  $\text{Fe}_3\text{O}_4$  nanoparticles were finally obtained.

### Analytical methods

#### X-ray diffraction

The  $\text{Fe}_3\text{O}_4$  nanoparticles were analyzed for phase composition using X-ray powder diffraction (XRD, Philips X'Pert PRO) over the  $2\theta$  range from  $10\text{--}90^\circ$  at rate of  $2.5^\circ/\text{min}$ , using  $\text{Cu-K}\alpha$  radiation ( $\lambda = 1.54060 \text{ \AA}$ ).

#### TEM and particle size analyzer

The morphology and size of the synthesized particles were observed using transmission electron microscope (TEM, HITACHI H-700H) at an accelerating voltage of 150 kV. Samples were prepared by placing drops of diluted ethanol dispersed of nanocrystalline on the surface of copper grids, which were purchased commercially. And size distribution was determined by Particle Size Analyzer (ZETA-SIZER, MALVERN Nano-ZS90).

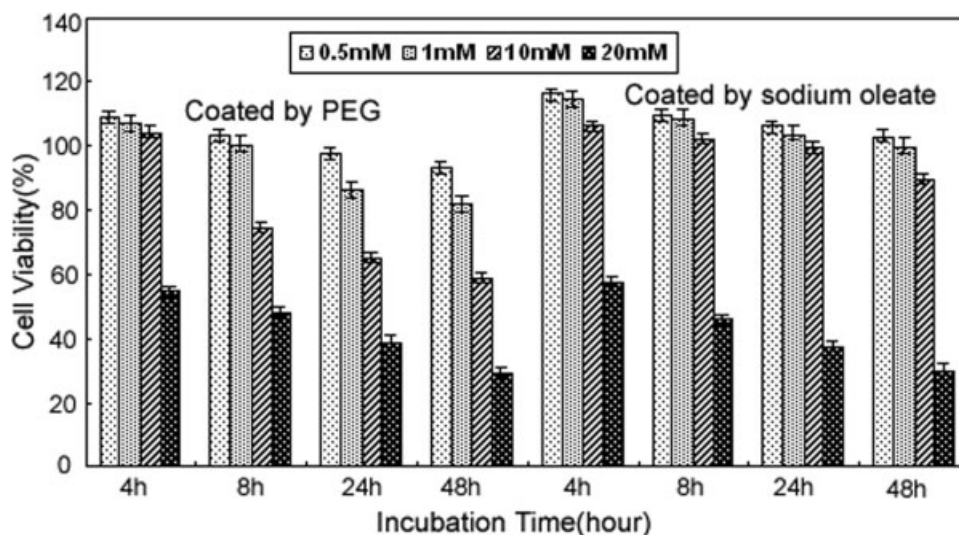


**Figure 1.** Cytotoxicity of Fe<sub>3</sub>O<sub>4</sub> nanoparticles coated by PEG (left) and sodium oleate (right) with different concentrations and different time.

## VSM

The magnetic properties of the resultant Fe<sub>3</sub>O<sub>4</sub> nanoparticles were measured with a vibrating sample magnetometer (VSM, Quantum Design) at room temperature.

## FT-IR

Fourier transform infrared spectrometer (FT-IR, Nicolet 5700) was performed to analyze the surface characteristics of the nanoparticles.

## MTT Assay and histochemistry analysis

To evaluate the cytotoxicity of Fe<sub>3</sub>O<sub>4</sub> nanoparticles, the 5-dimethylthiazol-2-yl-2,5-diphenyltetrazolium bromide (MTT) assay was performed as previously reported.<sup>10,11</sup> 3T3 monkey cells were cultured in Dulbecco's modified Eagle's medium (DMEM) supplemented with 10% fetal bovine serum (FBS) at 37°C in a 5% CO<sub>2</sub> incubator. For the cytotoxicity test, 3T3 cells were seeded at a density of  $20 \times 10^4$  cells/mL and 100  $\mu$ L/well in a 24-well flat bottomed microassay plates and incubated for 24 h before the addition of Fe<sub>3</sub>O<sub>4</sub> nanoparticles. After 24 h, Fe<sub>3</sub>O<sub>4</sub> nanoparticles were added to the cells in triplicate with final concentrations ranging from 0.5 to 20 mM (iron cations concentration) for 4–48 h. The cells were washed twice with PBS and replenished with fresh medium. Then, absorbance was measured at 570 nm using a Bio-Tek EL-311 microplate reader. The cell viability (%) was calculated according to the following Eq. (1):

$$\text{Cell viability (\%)} = \frac{\text{OD}_{570(\text{sample})}}{\text{OD}_{570(\text{control})}} \times 100 \quad (1)$$

where OD<sub>570(sample)</sub> represents the optical density of the wells treated with various concentration of iron cations, and OD<sub>570(control)</sub> represents that of the wells treated with DMEM + 10% FBS.

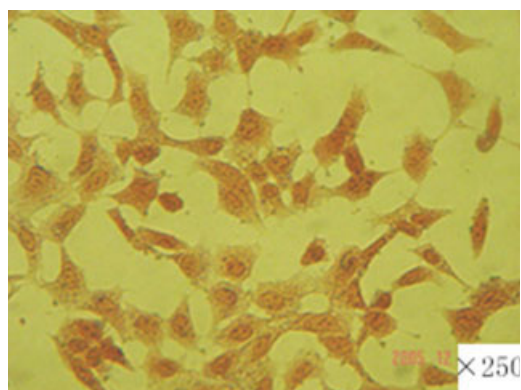
Histochemistry analysis was also performed as previously reported.<sup>10</sup> Prussian blue staining was used to reveal the presence of iron cations. Then, cells were fixed with 3% formaldehyde and washed with PBS, followed by incubation with 2% potassium ferrocyanide in 6% hydrochloric acid for 25 min. After wash, they were counterstained with neutral red solution. The samples were then examined under a light microscope.

## RESULTS

### MTT assay and histochemistry analysis of Fe<sub>3</sub>O<sub>4</sub> nanoparticles coated by PEG and sodium oleate respectively

Figure 1 shows the cell viability after incubation with different concentrations of Fe<sub>3</sub>O<sub>4</sub> nanoparticles coated by PEG and sodium oleate respectively. Over 90 and 70% cell viability was still obtained after 24-h incubation with 10 mM of Fe<sub>3</sub>O<sub>4</sub> nanoparticles coated by sodium oleate and PEG respectively. However, when the concentration of Fe<sub>3</sub>O<sub>4</sub> nanoparticles was 20 mM, the cell viability was lower than 60% as to the two kinds of samples even though the incubation time was just 4 h. After 24-h incubation, the cell viability would be lower than 40% as to the two kinds of samples when the concentration of Fe<sub>3</sub>O<sub>4</sub> nanoparticles was 20 mM. The results showed that Fe<sub>3</sub>O<sub>4</sub> nanoparticles coated by sodium oleate or PEG had low toxicity when the concentration of Fe<sub>3</sub>O<sub>4</sub> nanoparticles was lower than 10 mM, and the toxicity of Fe<sub>3</sub>O<sub>4</sub> nanoparticles coated by sodium oleate was lower than Fe<sub>3</sub>O<sub>4</sub> nanoparticles coated by PEG.

Figure 2(a) shows the Prussian blue staining of 3T3 cells for 4-h incubation, and Figure 2(b) shows that



(a)



(b)

**Figure 2.** (a) Prussian blue staining of 3T3 cells for 4-h incubation. (b) Prussian blue staining of 3T3 cells contained  $\text{Fe}_3\text{O}_4$  nanoparticles (2 mM) coated by sodium oleate in the cytoplasm for 4-h incubation. [Color figure can be viewed in the online issue, which is available at [www.interscience.wiley.com](http://www.interscience.wiley.com).]

Prussian blue staining of 3T3 cells contained  $\text{Fe}_3\text{O}_4$  nanoparticles (2 mM) coated by sodium oleate in the cytoplasm for 4-h incubation. From the two pictures, we can find that there was no obviously change in the quantity and shape of 3T3 cells, which showed that the cell viability was well, so  $\text{Fe}_3\text{O}_4$  nanoparticles coated by sodium oleate can be considered to be biocompatible.

#### The physical and magnetic properties of magnetite nanoparticles coated by different surfactant

Two different ferrofluid systems with the coating agents sodium oleate and polyethylene glycol (PEG,  $M_w = 6000$ ) were prepared and analyzed according to their physical and magnetic properties.

The XRD measurements indicated that magnetite ( $\text{Fe}_3\text{O}_4$ ) was the dominant phase for the two samples.

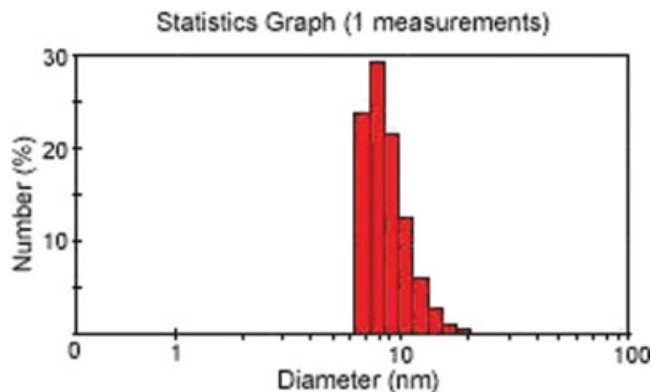


**Figure 3.** Particle size distribution of magnetite nanoparticles coated by sodium oleate described as number percent (%). [Color figure can be viewed in the online issue, which is available at [www.interscience.wiley.com](http://www.interscience.wiley.com).]

The mean size/size distribution was obtained from particle size analyzer, which are shown in Figures 3 and 4. As seen in Figures 3 and 4, particle sizes and sizes distribution are almost similar as the two samples, since identical processing conditions were used during the synthesis of the different samples. The TEM images also reveal a nearly spherical shape of the two samples. However, the concentration of polyethylene glycol (PEG-6000) was required to be more than 20% if we wanted to attain the magnetite nanoparticles whose sizes were smaller than 20 nm. As this, it increased the difficulty of washing and preparation of the samples, which were measured by transmission electron microscope (TEM) and particle size analyzer. Also, the cost of magnetite nanoparticles coated by PEG-6000 increased as the using of a mass of PEG-6000.

Then the saturation magnetization ( $M_s$ ) of the different samples was measured with a vibrating sample

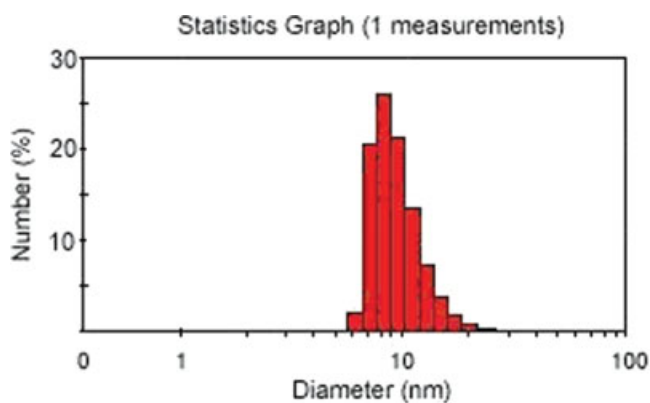


**Figure 4.** Particle size distribution of magnetite nanoparticles coated by PEG-6000 described as number percent (%). [Color figure can be viewed in the online issue, which is available at [www.interscience.wiley.com](http://www.interscience.wiley.com).]

**TABLE I**  
**Saturation Magnetization (Ms) of Different Samples**  
**with Mean Size Ranging from 10–20 nm**

Mean Sizes (nm)	Ms (emu/g)	
	Sodium oleate	PEG
10	42.31	31.28
15	44.73	33.51
20	49.23	39.67

magnetometer (VSM). The results are shown in Table I. As shown in Table I, the saturation magnetization (Ms) of magnetite nanoparticles increased as the sizes increased. And the saturation magnetization (Ms) of the magnetite nanoparticles coated by sodium oleate was greater than magnetite nanoparticles coated by PEG-6000 when they were measured with the same sizes. It reveals that the magnetic properties of magnetite nanoparticles coated by sodium oleate are better than magnetite nanoparticles coated by PEG.

According to the previous part, the magnetite nanoparticles coated by sodium oleate have a better biocompatibility, better magnetic properties, easier washing, and lower cost. Also, the Fe<sub>3</sub>O<sub>4</sub> nanoparticles can be well dispersed in an aqueous solution as the presence of COO<sup>-</sup> at the surface of magnetite nanoparticles. Taking into account the previous discussion, we chose sodium oleate as the apt surfactant. And the following results and discussion are all related to the magnetite nanoparticles coated by sodium oleate.

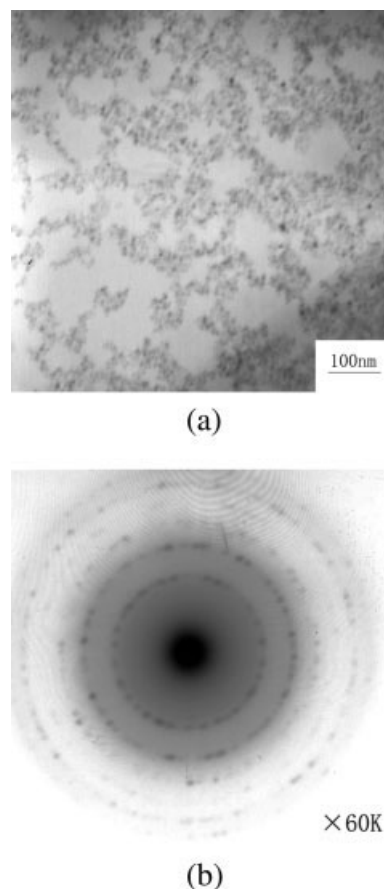
### TEM and ED image of Fe<sub>3</sub>O<sub>4</sub> nanoparticles

Figure 5(a) shows the typical transmission electron microscope (TEM) image of Fe<sub>3</sub>O<sub>4</sub> nanoparticles, from which we can see that the sizes of Fe<sub>3</sub>O<sub>4</sub> nanoparticles are almost uniform and most of Fe<sub>3</sub>O<sub>4</sub> nanoparticles are approximately spherical with the mean diameters (D<sub>v</sub>) of 8 nm. Figure 5(b) shows the electron diffraction pattern (ED) image of Fe<sub>3</sub>O<sub>4</sub> nanoparticles, which confirms that the sample is crystal and have an inverse cubic spinel structure.<sup>2,12–14</sup>

### X-ray power diffraction

Figure 6 shows the XRD pattern of the sample, which is quite identical to pure magnetite and matched well with that of it (JCPDS No. 82-1533), indicating that the sample has a cubic crystal system.<sup>15,16</sup> Also, we can see that no characteristic peaks of impurities were observed.

The mean particle diameters were also calculated from the XRD pattern according to the linewidth



**Figure 5.** (a) TEM image of Fe<sub>3</sub>O<sub>4</sub> nanoparticles. (b) ED pattern of Fe<sub>3</sub>O<sub>4</sub> nanoparticles.

of the (3 1 1) plane refraction peak using Scherrer Eq. (2):

$$D_c = \frac{K\lambda}{b \cos \theta} \quad (2)$$

The equation uses the reference peak width at angle  $\theta$ , where  $\lambda$  is the X-ray wave length (1.54060 Å),  $b$  is the width of the XRD peak at half height and  $K$  is a

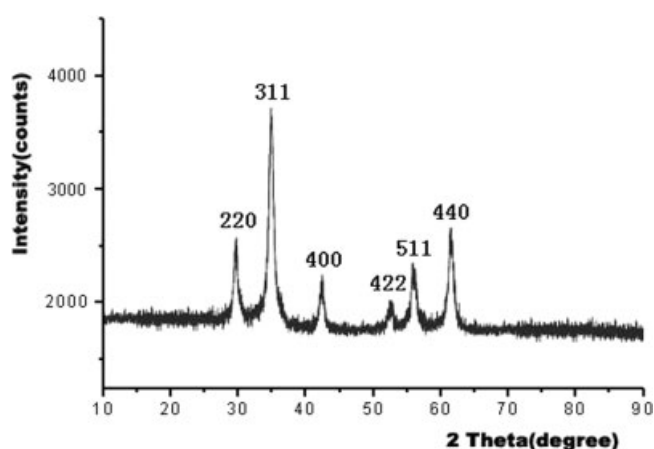


**Figure 6.** XRD pattern of Fe<sub>3</sub>O<sub>4</sub> nanoparticles.

**TABLE II**  
Mean Particle Sizes Determined by XRD and TEM

Coating Agents	$D_c$ (XRD) (nm)	$D_v$ (TEM) (nm)
Sodium oleate	7.1	8.0
PEG	7.3	8.5

shape factor, about 0.89 for magnetite. The results were coincident with the results obtained from the TEM analysis (Table II). However, the particle diameters from TEM measurements are slightly larger than the observed crystal sizes from XRD, due to the presence of noncrystalline surface layers.<sup>12,16</sup>

### FT-TR spectra of Fe<sub>3</sub>O<sub>4</sub> nanoparticles

In Figure 7(a), the peak at  $\sim 3439.4$  cm<sup>-1</sup> is attributed to the stretching vibrations of —OH, which is assigned to OH<sup>-</sup> absorbed by Fe<sub>3</sub>O<sub>4</sub> nanoparticles. And the peak at  $\sim 584.3$  cm<sup>-1</sup> is attributed to the Fe—O bond vibration of Fe<sub>3</sub>O<sub>4</sub>.<sup>12,13</sup> In Figure 7(b), the peak at  $\sim 3430.2$  cm<sup>-1</sup> is attributed to the stretching vibrations of —OH, which is also assigned to OH<sup>-</sup> absorbed by Fe<sub>3</sub>O<sub>4</sub> nanoparticles. The peaks at  $\sim 2924.2$  and  $\sim 2854.6$  cm<sup>-1</sup> are attributed to the stretching vibrations of —CH<sub>2</sub> and —CH<sub>3</sub> in sodium oleate. The peak at 1702.4 cm<sup>-1</sup> is assigned to the vibration of C=O in sodium oleate. The peak at 1590.3 cm<sup>-1</sup> is assigned to the vibration of C=C in sodium oleate. The peaks at 1472.5 and 1412.2 cm<sup>-1</sup> are attributed to the vibration of —CH. These all confirm that sodium oleate is absorbed in the surface of Fe<sub>3</sub>O<sub>4</sub> nanoparticles. And the peak at 578.4 cm<sup>-1</sup> is assigned to the Fe—O bond vibration of Fe<sub>3</sub>O<sub>4</sub> nanoparticles, we can see that

there is a little removal as to the peak in Figure 7(a), which is attributed to the presence of sodium oleate.<sup>12,13,17</sup>

## DISCUSSION

### Effect of different parameters determining the size/size distribution of Fe<sub>3</sub>O<sub>4</sub> nanoparticles

The concentration of sodium oleate solution

In this part, the reaction temperature was chosen as 50°C, the pH of the reaction solution was chosen as 10, and the stirring rate of the reaction system was chosen as 800 rpm. Figure 8 shows that the sizes of Fe<sub>3</sub>O<sub>4</sub> nanoparticles reduce with the increasing concentration of sodium oleate in the reaction system. This may be due to the fact that sodium oleate coats prevent magnetic particles reuniting so as to obtain particles with nanosize. It reveals that the sizes of Fe<sub>3</sub>O<sub>4</sub> nanoparticles can be well controlled as the dispersion action of sodium oleate, which can well control the growth of Fe<sub>3</sub>O<sub>4</sub> nucleus. However, when the concentration of sodium oleate is more than 3%, the sizes of Fe<sub>3</sub>O<sub>4</sub> nanoparticles are almost not changed. It indicates that Fe<sub>3</sub>O<sub>4</sub> nanoparticles have been almost stable when the concentration of sodium oleate arrives at 3%.

The reaction temperature

In this part, the concentration of sodium oleate in reaction system was chosen as 3%, the pH of the reaction system was chosen as 10, and the stirring rate of the

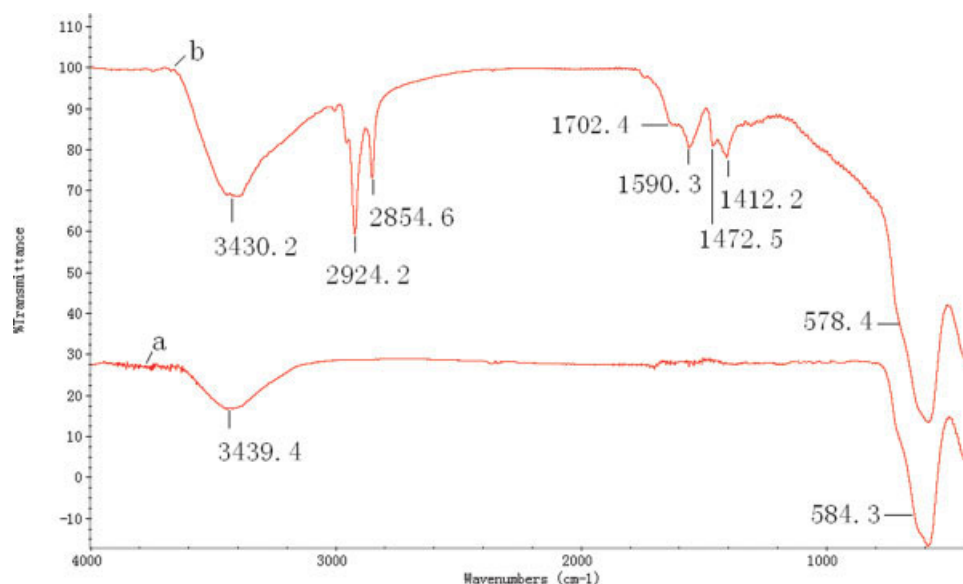


**Figure 7.** (a) FT-IR spectra of pure Fe<sub>3</sub>O<sub>4</sub> nanoparticles (b) Fe<sub>3</sub>O<sub>4</sub> nanoparticles modified with sodium oleate. [Color figure can be viewed in the online issue, which is available at [www.interscience.wiley.com](http://www.interscience.wiley.com).]

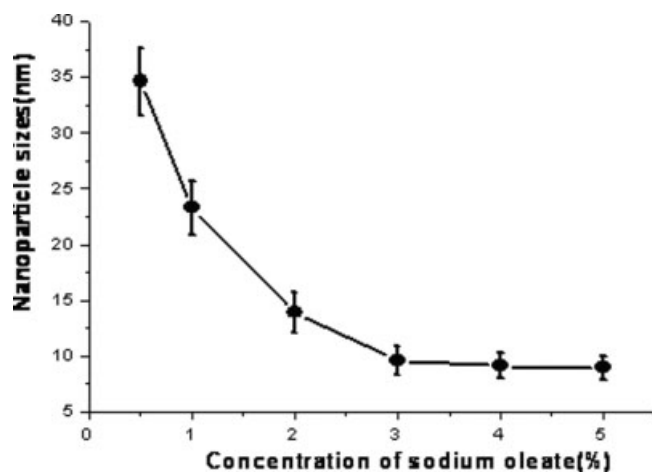


**Figure 8.** Effect of concentration of sodium oleate on size of Fe<sub>3</sub>O<sub>4</sub> nanoparticles.

reaction system was chosen as 800 rpm. From Figure 9, the sizes of Fe<sub>3</sub>O<sub>4</sub> nanoparticles reduce with the increase of reaction temperature when the reaction temperature is lower than 50°C, while the sizes of Fe<sub>3</sub>O<sub>4</sub> nanoparticles enlarge with the increase of the reaction temperature when the reaction temperature is higher than 50°C. Increasing the reaction temperature enhanced both the rate of adsorption of sodium oleate and the viscosity of the coat phase. All these factors would reduce the extent of aggregation of Fe<sub>3</sub>O<sub>4</sub> nucleus and reduce sizes of Fe<sub>3</sub>O<sub>4</sub> particles. However, the growth of Fe<sub>3</sub>O<sub>4</sub> nucleus is easier to happen when the temperature is higher than 50°C, resulting in larger size nanoparticles when the temperature is higher than 50°C.

#### pH of the reaction solution

In this part, the concentration of sodium oleate in the reaction system was chosen as 3%, the reaction temperature of the reaction system was chosen as

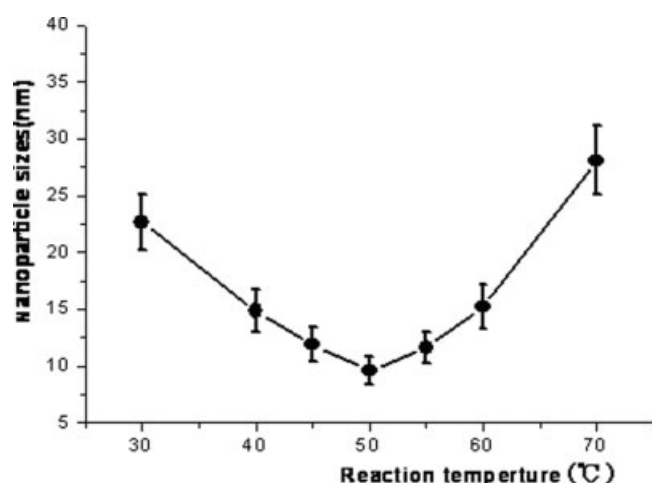


**Figure 9.** Effect of reaction temperature on sizes of Fe<sub>3</sub>O<sub>4</sub> nanoparticles.

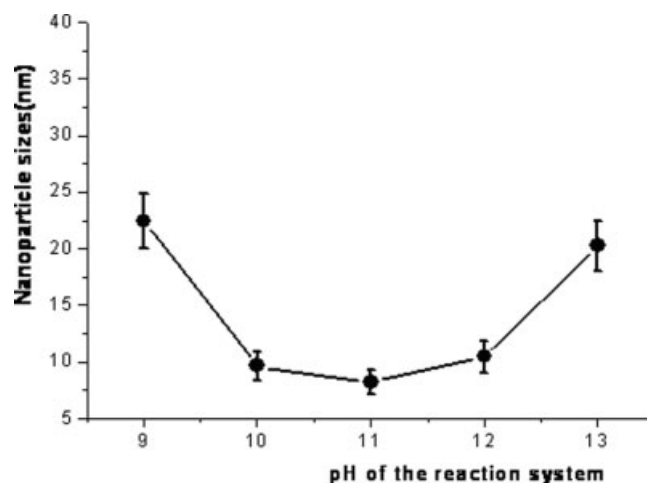
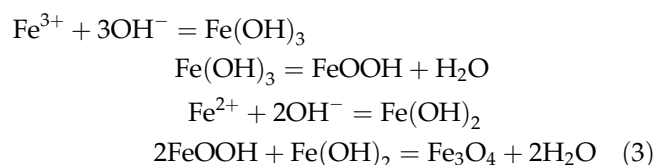


**Figure 10.** Effect of the solution pH on sizes of Fe<sub>3</sub>O<sub>4</sub> nanoparticles.

50°C, and the stirring rate of the reaction system was chosen as 800 rpm. From Figure 10, the sizes of Fe<sub>3</sub>O<sub>4</sub> nanoparticles reduce with the increase of solution pH when the pH is lower than 11, while the mean diameter of Fe<sub>3</sub>O<sub>4</sub> nanoparticles increase with the increase of solution pH when the pH is higher than 11. And there is a remarkable increase when the solution pH is increased from 12 to 13. The reason can be explained by the forming mechanism of magnetite:<sup>2</sup>



When the pH of the reaction system increases, Fe(OH)<sub>3</sub> generated in the first step, which was owing

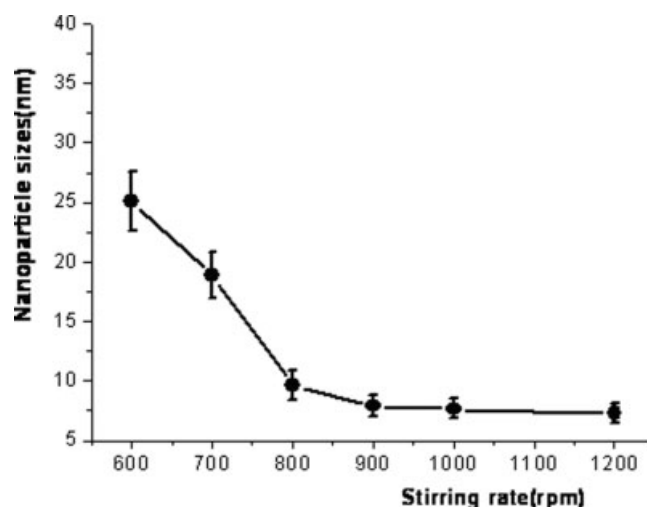


**Figure 11.** Effect of the stirring rate on sizes of Fe<sub>3</sub>O<sub>4</sub> nanoparticles.

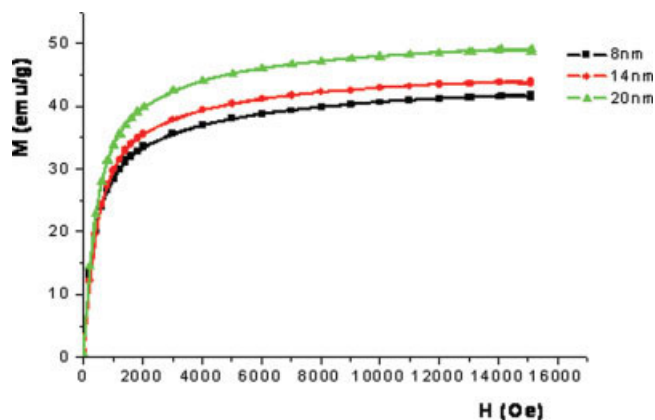


**Figure 12.** Effect of the sizes on the magnetization properties of  $\text{Fe}_3\text{O}_4$  nanoparticles. [Color figure can be viewed in the online issue, which is available at [www.interscience.wiley.com](http://www.interscience.wiley.com).]

to the hydrolysis of  $\text{Fe}^{3+}$ . Then,  $\text{Fe}(\text{OH})_2$  generated as pH of the reaction system increased, which was owing to the hydrolysis of  $\text{Fe}^{2+}$ . Finally  $\text{Fe}_3\text{O}_4$  just can be formed as more increase of the solution pH.<sup>2</sup> It reveals that the nucleation of  $\text{Fe}_3\text{O}_4$  nucleus is easier to happen when the solution pH is lower than 11, while the growth of  $\text{Fe}_3\text{O}_4$  nucleus is easier to happen when the solution pH is higher than 11.

The stirring speed of the reaction system

In this part, the concentration of sodium oleate in reaction system was chosen as 3%, the pH of the reaction system was chosen as 10 and the reaction temperature was chosen as  $50^\circ\text{C}$ . From Figure 11, we can see that the sizes of  $\text{Fe}_3\text{O}_4$  nanoparticles reduce with increase of stirring speed of the reaction system. This trend can be explained by the energy transfer differences for the different stirring rates: when the stirring rate is increased, the energy transferred to the suspension medium is increased and the reaction solution can be dispersed into smaller droplets and the size is reduced.

However, the sizes of  $\text{Fe}_3\text{O}_4$  nanoparticles are almost not changed when the stirring speed is higher than 900 rpm. And from the experiment, we can see that a great deal of bubbles would generate and there would be splashing of the reaction solution, when the stirring speed was higher than 900 rad/min. Also  $\text{Fe}_3\text{O}_4$  nanoparticle will be easily oxidized. So 900 rpm can be considered as the best stirring speed as to this reaction system.

Magnetization properties of magnetite nanoparticles with different sizes

The magnetization curve for  $\text{Fe}_3\text{O}_4$  nanoparticles is shown in Figure 12. As we can see, the magnetization

curve is to be without hysteresis, the coercivity field and remnant magnetization cannot be found from the curve. It confirms that  $\text{Fe}_3\text{O}_4$  nanoparticles are characteristic of superparamagnetic properties. From the magnetization curve, we can also see that the saturation magnetization ( $M_s$ ) of the  $\text{Fe}_3\text{O}_4$  nanoparticles increase from 41.60 to 49.24 emu/g when the sizes of magnetite increase from 8 to 20 nm, which can be attributed to the increase of weight and volume of magnetite nanoparticles. According to the study, the magnetic properties are well through they are lower than that of the bulk phase (88 emu/g).<sup>17–19</sup>

## CONCLUSIONS

Ultrafine, uniform, nearly spherical, and high purity  $\text{Fe}_3\text{O}_4$  nanoparticles could be prepared by the controlled chemical coprecipitation method from the solution of ferrous/ferric mixed salt-solution in aqueous ammonium hydroxide ( $\text{NH}_3\cdot\text{H}_2\text{O}$ ) solution when sodium oleate was chosen as the apt surfactant. The  $\text{Fe}_3\text{O}_4$  nanoparticles have a perfect biocompatibility and can also be well dispersed in an aqueous solution as the presence of  $\text{COO}^-$  at the surface of magnetite nanoparticles. The results show that  $\text{Fe}_3\text{O}_4$  nanoparticles can be produced in the sizes range from 8 to 20 nm by changing the operational parameters (i.e., concentration of sodium oleate, reaction temperature, solution pH, and stirring rate). The saturation magnetization ( $M_s$ ) of the magnetite nanoparticles increased from 41.60 to 49.24 emu/g, and the magnetic field intensity for the magnetite nanoparticles was in the range 8000–15,000 Oe, which shows that the magnetic properties of the  $\text{Fe}_3\text{O}_4$  nanoparticles are preferable.<sup>20,21</sup> From the previous part,  $\text{Fe}_3\text{O}_4$  nanoparticles, which were prepared by the previous method, can be promising as a potentially good magnetic support to be employed in magnetic carrier technology with good economical aspects, good biocompatibility, and good magnetic quality.

## References

1. Häfeli U, Schütt W, Teller J, Zborowski M. *Scientific and Clinical Applications of Magnetic Microspheres*. New York: Plenum; 1997.
2. Lian S, Wang E, Kang Z, Bai Y, Gao L, Jiang M, Hu C, Xu L. Synthesis of magnetite nanorods and porous hematite nanorods. *Solid State Commun* 2004;129:485–490.
3. Zaitsev VS, Filimonov DS, Presnyakov IA, Gambino RJ, Chu B. Physical and chemical properties of magnetite and magnetite-polymer nanoparticles and their colloidal dispersions. *J Colloid Interface Sci* 1999;212:49–57.
4. Lian S, Kanga Z, Wang E, Jiang M, Hu C, Xu L. Convenient synthesis of single crystalline magnetic  $\text{Fe}_3\text{O}_4$  nanorods. *Solid State Commun* 2003;127:605–608.
5. Sun Y-K, Ma M, Zhang Y, Gu N. Synthesis of nanometer-size maghemite particles from magnetite. *Colloids Surf A: Physicochem Eng Aspects* 2004;245:15–19.



6. Cornell RM, Schertmann U. Iron Oxides in the Laboratory: Preparation and Characterization. Weinheim: VCH; 1991.
7. Chen S, Feng J, Guo X, Hong J, Ding W. One-step wet chemistry for preparation of magnetite nanorods. *Mater Lett* 2005;59:985–988.
8. Bae D-S, Han K-S, Cho S-B, Choi S-H. Synthesis of ultrafine Fe<sub>3</sub>O<sub>4</sub> powder by glycothermal process. *Mater Lett* 1998;37:255–258.
9. Kim DK, Zhang Y, Voit W, Rao KV, Muhammed M. Synthesis and characterization of surfactant-coated superparamagnetic monodispersed iron oxide nanoparticles. *J Magn Magn Mater* 2001;225:30–36.
10. Cheng F-Y, Su C-H, Yang Y-S, Yeh C-S, Tsai C-Y, Wu C-L, Wu M-T, Shieh D-B. Characterization of aqueous dispersions of Fe<sub>3</sub>O<sub>4</sub> nanoparticles and their biomedical applications. *Biomaterials* 2005;26:729–738.
11. Yang Y, Jia W, Qi X, Yang C, Liu L, Zhang Z, Zhou S. Novel biodegradable polymers as gene carriers. *Macromol Biosci* 2004;4:1113–1117.
12. Cornell RM, Schwertmann U. The Iron Oxide: Structure, Properties, Reactions, Occurrence and Uses. Weinheim: VCH; 1996.
13. Ma M, Zhang Y, Yu W, Shen H-Y, Zhang H-Q, Gu N. Preparation and characterization of magnetite nanoparticles coated by amino silane. *Colloids Surf A: Physicochem Eng Aspects* 2003;212:219–226.
14. Chen S, Feng J, Guo X, Hong J, Ding W. One-step wet chemistry for preparation of magnetite nanorods. *Mater Lett* 2005;59:985–998.
15. Itoh H, Sugimoto T. Systematic control of size, shape, structure, and magnetic properties of uniform magnetite and maghemite particles. *J Colloid Interface Sci* 2003;265:283–295.
16. Voit W, Kim DK, Zapka W, Muhammed M, Rao KV. Magnetic behavior of coated superparamagnetic iron oxide nanoparticles in ferrofluids. *Mater Res Soc* 2001;676:781–786.
17. Huang Z, Tang F. Preparation, structure, and magnetic properties of mesoporous magnetite hollow spheres. *J Colloid Interface Sci* 2005;281:432–436.
18. Gomez-Lopera SA, Plaza RC, Delgado AV. Synthesis and characterization of spherical magnetite/biodegradable polymer composite particles. *J Colloid Interface Sci* 2001;240:40–47.
19. Jiang W, Yang HC, Yang SY, Horng HE, Hung JC, Chen YC, Hong C-Y. Preparation and properties of superparamagnetic nanoparticles with narrow size distribution and biocompatible. *J Magn Magn Mater* 2004;283:210–214.
20. Denkbaz EB, Kilicay E, Birlikseven C, Öztürk E. Magnetic chitosan microspheres: Preparation and characterization. *React Funct Polym* 2002;50:225–232.
21. Avivi S, Felner I, Novik I, Gedanken A. The preparation of magnetic proteinaceous microspheres using the sonochemical method. *Biochim Biophys Acta* 2001;1527:123–129.